J. Fluid Mech. (1971), *vol.* 45, *part* 4, *pp.* 659–671
Printed in Great Britain

Baroclinic stability under non-hydrostatic conditions

By PETER H. STONE
Division of Engineering and Applied Physics, Harvard University

(Received 20 April 1970)

Eady's model for the stability of a thermal wind in an inviscid, stratified, rotating system is modified to allow for deviations from hydrostatic equilibrium. The stability properties of the flow are uniquely determined by two parameters: the Richardson number Ri, and the ratio of the aspect ratio to the Rossby number δ. The latter parameter may be taken as a measure of the deviations from hydrostatic equilibrium ($\delta = 0$ in Eady's model). It is found that such deviations decrease the growth rates of all three kinds of instability which can occur in this problem: 'geostrophic' baroclinic instability, symmetric instability, and Kelvin–Helmholtz instability. The unstable wavelengths for 'geostrophic' and Kelvin–Helmholtz instability are increased for finite values of δ, while the unstable wavelengths for symmetric instability are unaffected. The 'non-hydrostatic' effects ($\delta \neq 0$) are significant for symmetric and Kelvin–Helmholtz instability when $\delta \gtrsim 1$, but not for 'geostrophic' instability unless $\delta \gg 1$. Consequently, the first two types of instability tend to be suppressed relative to 'geostrophic' instability by 'non-hydrostatic' conditions. Figure 3 summarizes the different instability régimes that can occur. In laboratory experiments symmetric instability can be studied best when $\delta \lesssim 1$, while Kelvin–Helmholtz instability can be studied best when $\delta \ll 1$.

1. Introduction

In most geophysical problems the assumption of hydrostatic equilibrium is a good one, and consequently discussions of baroclinic stability generally proceed from this assumption (see, for example, Phillips 1963). However, the development of the theory of baroclinic stability has been greatly aided by experimental studies of baroclinic stability (for example, see, Fultz *et al.* 1959, and Fowlis & Hide 1965), and in these studies the assumption of hydrostatic equilibrium is not such a good one. If the motions are geostrophic, then the vertical motions are relatively weak and hydrostatic equilibrium will be favoured even in the experiments, but this is still no guarantee of hydrostatic equilibrium if the aspect ratio is sufficiently large. In addition some recent experiments have been specifically oriented towards the non-geostrophic problem (Stone *et al.* 1969). Consequently, in this paper we present an analysis of how non-hydrostatic conditions will affect the various kinds of instability which can arise in a baroclinic zonal flow.

2. Mathematic model

For our study we will use the model first introduced by Eady (1949), but with the one difference that we will not assume hydrostatic equilibrium. Therefore we assume a Boussinesq adiabatic inviscid fluid with density ρ and thermal expansion coefficient α located on a plane rotating about a vertical axis with angular speed Ω, and with an acceleration of gravity g. If x, y and z are respectively the zonal, meridional, and vertical rectangular co-ordinates, and t the time, then the conservation equations for the zonal velocity u, the meridional velocity v, the vertical velocity w, the pressure P, and the temperature T, are

$$\frac{\partial u}{\partial x}+\frac{\partial v}{\partial y}+\frac{\partial w}{\partial z}=0, \tag{2.1}$$

$$\frac{du}{dt}=2\Omega v-\frac{1}{\rho}\frac{\partial P}{\partial x}, \tag{2.2}$$

$$\frac{dv}{dt}=-2\Omega u-\frac{1}{\rho}\frac{\partial P}{\partial y}, \tag{2.3}$$

$$\frac{dw}{dt}=-\frac{1}{\rho}\frac{\partial P}{\partial z}+\alpha g T, \tag{2.4}$$

$$\frac{dT}{dt}=0. \tag{2.5}$$

We assume that the fluid is contained between two horizontal planes at $z=0, H$ and is unbounded horizontally, so that the boundary conditions are

$$w=0 \quad \text{at} \quad z=0, H. \tag{2.6}$$

Our basic flow state will consist of a zonal wind of magnitude u_0 with constant vertical shear and no horizontal shear, and a temperature field with constant stratification $\partial\overline{T}/\partial z$ and a constant horizontal gradient related to u_0 by the thermal wind relation. It is convenient to use dimensionless variables, and, in order to put the equations in dimensionless form, we will use the following basic units: $x \sim u_0/2\Omega$, $y \sim u_0/2\Omega$, $z \sim H$, $t \sim 1/2\Omega$, $u \sim u_0$, $v \sim u_0$, $w \sim 2\Omega H$, $T \sim H\partial\overline{T}/\partial z$, and $P \sim \alpha\rho g H^2 \partial\overline{T}/\partial z$. Equations (2.1)–(2.6), now in terms of the *dimensionless* variables, become

$$\frac{\partial u}{\partial x}+\frac{\partial v}{\partial y}+\frac{\partial w}{\partial z}=0, \tag{2.7}$$

$$\frac{du}{dt}=v-Ri\frac{\partial P}{\partial x}, \tag{2.8}$$

$$\frac{dv}{dt}=-u-Ri\frac{\partial P}{\partial y}, \tag{2.9}$$

$$\delta^2\frac{dw}{dt}=-Ri\frac{\partial P}{\partial z}+RiT, \tag{2.10}$$

$$\frac{dT}{dt}=0, \tag{2.11}$$

$$w=0 \quad \text{on} \quad z=0,1. \tag{2.12}$$

Two dimensionless parameters appear, the Richardson number,

$$Ri = \frac{\alpha g H^2}{u_0^2}\frac{\partial \overline{T}}{\partial z}, \tag{2.13}$$

and

$$\delta = 2\Omega H/u_0. \tag{2.14}$$

The parameter δ is the ratio of the aspect ratio H/L to the Rossby number $u_0/2\Omega L$, with L being any appropriate horizontal scale. The basic flow state in terms of the dimensionless variables is

$$v = w = 0, \tag{2.15}$$

$$u = z, \tag{2.16}$$

$$T = z - \frac{y}{Ri} + \text{constant}, \tag{2.17}$$

$$P = \tfrac{1}{2}z^2 - \frac{yz}{Ri} + \text{constant}. \tag{2.18}$$

Now we assume small deviations from this basic flow state, and linearize (2.7)–(2.12). The coefficients of the linearized equations depend only on z, so we can assume perturbation solutions of the form $\exp\{i(\sigma t + kx + \lambda y)\}$. The resulting equations for the z dependance of the dimensionless *perturbation* variables are

$$iku + i\lambda v + \frac{dw}{dz} = 0, \tag{2.19}$$

$$i(\sigma + kz)\,u + w = v - ik\,Ri\,P, \tag{2.20}$$

$$i(\sigma + kz)\,v = -u - i\lambda\,Ri\,P, \tag{2.21}$$

$$i\delta^2(\sigma + kz)\,w = -Ri\frac{dP}{dz} + Ri\,T, \tag{2.22}$$

$$i(\sigma + kz)\,T - \frac{v}{Ri} + w = 0, \tag{2.23}$$

$$w = 0 \quad \text{on} \quad z = 0, 1. \tag{2.24}$$

With a little algebra this set of equations can be reduced to a single eigenvalue equation for the perturbation vertical velocity,

$$[1-(\sigma+kz)^2]\frac{d^2w}{dz^2} - 2\left[\frac{k}{\sigma+kz} - i\lambda\right]\frac{dw}{dz} - \left[(k^2+\lambda^2)\,Ri - (k^2+\lambda^2)\,\delta^2(\sigma+kz)^2 + \frac{2i\lambda k}{\sigma+kz}\right]w = 0. \tag{2.25}$$

When $\delta = 0$ this equation reduces to Eady's (1949, equation II, 11). Since the unit of horizontal scale is $u_0/2\Omega$, the dimensionless wave-numbers k and λ are simply the zonal and meridional Rossby numbers of the perturbation.

The solutions of (2.25) under hydrostatic conditions ($\delta = 0$) have been studied in two previous papers (Stone 1966; Stone 1970), hereinafter referred to as I and II, respectively. The results show that three basically different types of instability can occur when $Ri > 0$: 'geostrophic' baroclinic instability of the kind first discovered by Charney (1947) and Eady (1949) (this type of instability is

actually only geostrophic if $Ri \gg 1$, but it is nevertheless conventional to refer to it as 'geostrophic'); symmetric instability of the kind discussed by Solberg (1936); and an instability analogous to the Kelvin–Helmholtz instability of two superposed layers of fluid with different velocities and densities (in Eady's model we have continuous variations of u and ρ). The numerical results of II showed that the analytical methods of I (namely, perturbation expansions of the solution to the eigenvalue problem in powers of k and λ) are adequate to study these different kinds of instability. Consequently, we shall here use the same method as in I, and in each of the next three sections we will consider how finite values of δ modify one of the different kinds of instability. Since $\delta = 0$ corresponds either to a zero aspect ratio or to an infinite Rossby number, finite values of δ may be taken as either a measure of the deviations from hydrostatic equilibrium, or as a measure of the deviations from a non-rotating state. The former point of view is preferable for 'geostrophic' and symmetric instability, while the latter is preferable for Kelvin–Helmholtz instability.

3. 'Geostrophic' instability

According to the results of I and II, the maximum growth rates for this kind of instability occur for perturbations that are independent of the meridional direction ($\lambda = 0$), have large zonal scales ($k \ll 1$), and have small growth rates ($\sigma \sim k$). Therefore, to find how these perturbations are modified under non-hydrostatic conditions, we set $\lambda = 0$, substitute

$$\sigma = kc \tag{3.1}$$

in (2.25), obtaining

$$[1-k^2(c+z)^2]\frac{d^2w}{dz^2} - \frac{2}{c+z}\frac{dw}{dz} - [k^2Ri - k^4\delta^2(c+z)^2]w = 0, \tag{3.2}$$

and then expand the solution in powers of k^2:

$$w = w_0 + k^2 w_1 + \ldots, \tag{3.3}$$

$$c = c_0 + k^2 c_1 + \ldots. \tag{3.4}$$

The results of II showed that when $\delta = 0$ the maximum growth rate and corresponding zonal wave-number could be obtained with an accuracy of 7 % or better if only the first two terms in the series (3.4) were retained. To find how these quantities are modified when $\delta \neq 0$, we shall also only retain the first two terms in (3.4). As we shall see below, the zonal wave-number corresponding to a maximum growth rate decreases when $\delta \neq 0$, so retaining only the first two terms will be an even better approximation when $\delta \neq 0$.

Examining (3.2), we see that, if $\delta \sim 1$, the non-hydrostatic effects are of order k^4, and therefore to a first approximation will not affect the most rapidly growing 'geostrophic' instabilities. Only if $\delta \gg 1$ will non-hydrostatic modifications become important. To determine these modifications we replace δ in (3.2) by the aspect ratio for the perturbation,

$$\epsilon = k\delta, \tag{3.5}$$

and assume that $\epsilon \sim 1$ when making the expansions (3.3) and (3.4).

The resulting eigenvalue equations for the first two terms in the expansion are

$$Lw_0 \equiv \frac{d^2w_0}{dz^2} - \frac{2}{c_0+z}\frac{dw_0}{dz} = 0, \tag{3.6}$$

$$Lw_1 = (c_0+z)^2\frac{d^2w_0}{dz^2} - \frac{2c_1}{(c_0+z)^2}\frac{dw_0}{dz} + [Ri - \epsilon^2(c_0+z)^2]w_0. \tag{3.7}$$

Integrating (3.6) and applying boundary condition (2.24) we find

$$w_0 = (c_0+z)^3 - c_0^3, \tag{3.8}$$

$$c_0 = -\tfrac{1}{2} \pm \frac{i}{2\sqrt{3}}. \tag{3.9}$$

We use the solubility condition, which follows from the definition of L and the boundary conditions on w_0 and w_1,

$$\int_0^1 \frac{w_0 Lw_1}{(c_0+z)^2}\,dz = 0, \tag{3.10}$$

to obtain from (3.7)

$$c_1 = \mp\frac{i}{15\sqrt{3}}\left(1 + Ri + \frac{5\epsilon^2}{42}\right). \tag{3.11}$$

From (3.4), (3.9) and (3.11), we find the approximate expression for the growth rate σ_i ($\sigma_i = -\operatorname{Im}\sigma$):

$$\sigma_i \cong \frac{1}{2\sqrt{3}}\left[k - \frac{2k^3}{15}\left(1 + Ri + \frac{5\delta^2k^2}{42}\right)\right]. \tag{3.12}$$

Equation (3.12) is plotted in figure 1 in order to illustrate how the growth rates of 'geostrophic' instabilities are modified under non-hydrostatic conditions. The curves were drawn for $Ri = 2$ (different values of Ri do not change the qualitative behaviour) and for $\delta = 0, 10, 40$. The unstable wave-numbers and the growth rates decrease for large values of δ. If we maximize σ_i as given by equation (3.12) with respect to k, we find that the most rapidly growing wave-number is given by

$$k_{\max}^2 \cong \frac{63}{10\delta^2}\left[-\tfrac{2}{5}(1+Ri) + \left\{\tfrac{4}{25}(1+Ri)^2 + \frac{20\delta^2}{63}\right\}^{\frac{1}{2}}\right]. \tag{3.13}$$

Under extreme non-hydrostatic conditions we find

$$\lim_{\delta\to\infty} k_{\max} = (\tfrac{63}{20})^{\frac{1}{4}}\left(\frac{2}{\delta}\right)^{\frac{1}{2}}, \tag{3.14}$$

and the corresponding maximum growth rate is

$$\lim_{\delta\to\infty} \sigma_{i\max} = \tfrac{2}{5}(\tfrac{63}{20})^{\frac{1}{4}}\left(\frac{2}{3\delta}\right)^{\frac{1}{2}}. \tag{3.15}$$

The most rapidly growing modes are not actually geostrophic when $Ri \lesssim 1$, $\delta \lesssim 1$, i.e. $k_{\max} \sim 1$. Nevertheless, neglecting the higher order terms in the expansion in powers of k^2 remains a good approximation (see II, figure 10, to obtain an idea of how the exact and approximate solutions differ).

The results of I and II showed that, for small enough values of Ri, the 'geostrophic' baroclinic instabilities lose their clear-cut identity. Specifically, the

growth rates of the perturbations with $\lambda \neq 0$ dominate over those with $\lambda = 0$; the perturbation $\lambda = 0$, $k = k_{\max}$ represents a saddle point of $\sigma_i(k, \lambda)$ instead of a local maximum; and there is no longer a sharp delineation between the 'geostrophic' instabilities and the more rapidly growing symmetric instabilities.

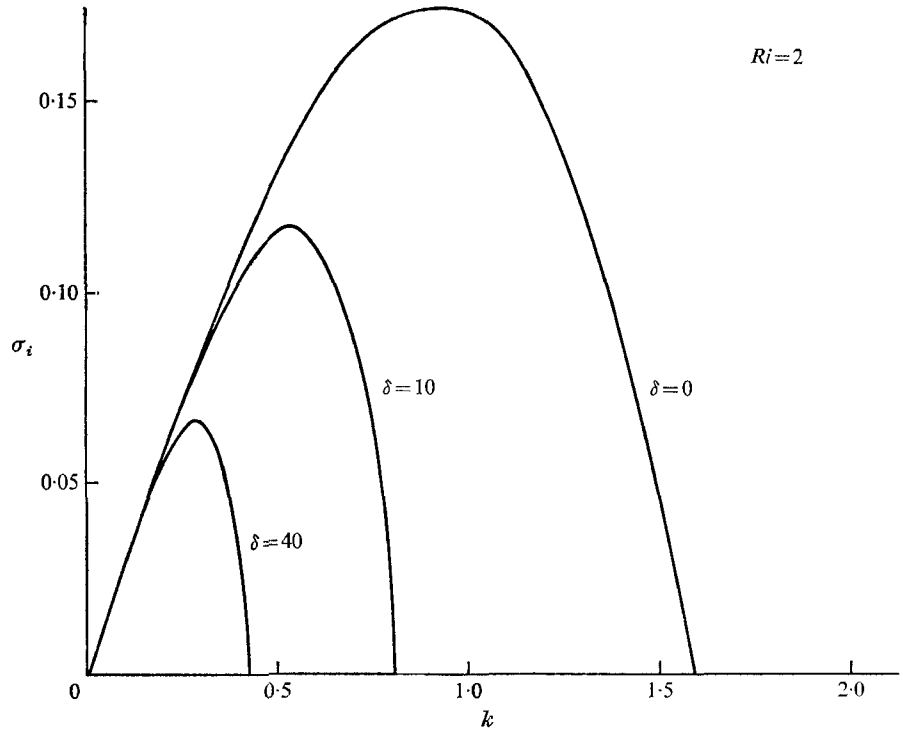

FIGURE 1. Growth rates against zonal wave-number for 'geostrophic' instabilities under hydrostatic ($\delta = 0$) and non-hydrostatic ($\delta = 10, 40$) conditions.

To determine under what conditions the two types of instability are distinct, we need to know whether σ_i increases or decreases as λ increases from zero. We may determine this to a first approximation by substituting $\sigma = kc$ into (2.25); replacing δ by ϵ; letting $k \to 0$ while assuming $\epsilon \sim 1$ so as to retain non-hydrostatic effects; and expanding the solution in powers of λ. If we perform these operations, but do not yet expand in λ, (2.25) becomes

$$\frac{d^2w}{dz^2} - 2\left[\frac{1}{c+z} - i\lambda\right]\frac{dw}{dz} - \left[\lambda^2 Ri^2 - \epsilon^2\lambda^2(c+z)^2 + \frac{2i\lambda}{c+z}\right]w = 0. \tag{3.16}$$

It is convenient to substitute into this equation

$$w = \exp\left[-i\lambda(c+z)\right]\psi, \tag{3.17}$$

so that the eigenvalue equation becomes

$$\frac{d^2\psi}{dz^2} - \frac{2}{c+z}\frac{d\psi}{dz} + \lambda^2[1 - Ri + \epsilon^2(c+z)^2]\psi = 0. \tag{3.18}$$

Now we expand the solution in powers of λ^2,

$$\left.\begin{aligned} \psi &= \psi_0 + \lambda^2\psi_1 + \ldots, \\ c &= c_0 + \lambda^2 c_1 + \ldots. \end{aligned}\right\} \tag{3.19}$$

The zero-order eigenvalue equation is again

$$L\psi_0 = 0, \tag{3.20}$$

so the zero-order solution for ψ_0 and c_0 is the same as that found for w_0 and c_0 in the k^2 expansion ((3.8) and (3.9)). The first-order eigenvalue equation is

$$L\psi_1 = \frac{-2c_1}{(c_0+z)^2}\frac{d\psi_0}{dz} - [1 - Ri + \epsilon^2(c_0+z)^2]\,\psi_0. \tag{3.21}$$

Again we find c_1 by applying condition (3.10) with ψ_0 and ψ_1 replacing w_0 and w_1. We obtain

$$c_1 = \mp\frac{i}{15\sqrt{3}}\left[Ri - 1 + \frac{5\epsilon^2}{42}\right]. \tag{3.22}$$

From (3.22) and (3.19) we see that the critical value of Ri is given by

$$Ri = 1 - \frac{5\epsilon^2}{42}. \tag{3.23}$$

For larger values of Ri, the perturbations $\lambda = 0$ have greater growth rates than the perturbations $0 < \lambda^2 \ll 1$, and consequently the 'geostrophic' instabilities are distinct. For smaller values of Ri, the perturbations $\lambda = 0$ have smaller growth rates, and the symmetric and 'geostrophic' instabilities are no longer distinct. The accuracy of the critical value given by (3.23) may be determined by comparing its value when $\epsilon = 0$, $Ri = 1$, with the exact value found in II, $Ri = 0{\cdot}84$. Since the maximum growth rates occur for smaller values of k when $\epsilon \neq 0$, neglecting the higher-order terms in k^2, in order to obtain (3.23), will be an even better approximation when $\epsilon \neq 0$. The critical value of Ri may be related directly to δ instead of ϵ, by substituting (3.13) for $k_{\max}$ into $\epsilon = \delta k$, and then substituting for ϵ in (3.23). We find

$$\delta^2 = \tfrac{56}{25}(1 - Ri)\,(4 - Ri). \tag{3.24}$$

Finally, we note that the eigenfunction for the most rapidly growing mode is changed little under non-hydrostatic conditions. The higher-order terms in the k^2 expansion are always relatively small for this mode. The second term in the expansion of w is largest when $\delta = 0$, and even then its amplitude never exceeds 31 % of the amplitude of the first term (w_1 is given in §4 of I). Consequently, (3.8) is a good approximation to the most rapidly growing mode for 'geostrophic' instability under all conditions.

4. Symmetric instabilities

The maximum growth rates for these instabilities are associated with the perturbations $k = 0, \lambda \gg 1$, and have growth rates $\sigma_i \sim 1$ (see I and II). Therefore, we can study their modifications under non-hydrostatic conditions by setting $k = 0$ in (2.25). The eigenvalue equation then becomes

$$(1 - \sigma^2)\frac{d^2w}{dz^2} + 2i\lambda\frac{dw}{dz} - \lambda^2(Ri - \sigma^2\delta^2)\,w = 0. \tag{4.1}$$

Its solutions, subject to boundary conditions (2.24), are

$$w = \exp\left\{\frac{-i\lambda z}{1-\sigma^2}\right\}\sin m\pi z, \tag{4.2}$$

$$\sigma^2 = (1+x^2\delta^2)^{-1}\left\{1+x^2\frac{Ri+\delta^2}{2} \pm \left[x^4\left(\frac{Ri+\delta^2}{2}\right)^2 + x^2 + x^4\delta^2(1-Ri)\right]^{\frac{1}{2}}\right\}, \tag{4.3}$$

where

$$x = \lambda/m\pi, \quad m = 1, 2, 3, \ldots. \tag{4.4}$$

Only those eigenvalues in (4.3) for which we choose the minus sign in front of the square root correspond to instability ($\sigma^2 < 0$). The growth rate is a maximum as $x \to \infty$, and in this limit

$$\lim_{x\to\infty} \sigma^2 = \frac{Ri+\delta^2-[(Ri+\delta^2)^2+4\delta^2(1-Ri)]^{\frac{1}{2}}}{2\delta^2}. \tag{4.5}$$

Therefore, symmetric instability can occur if and only if $Ri < 1$, regardless of the strength of the non-hydrostatic effects. The maximum growth rate under hydrostatic conditions is given by

$$\lim_{\substack{x\to\infty \\ \delta\to 0}} \sigma^2 = 1 - \frac{1}{Ri}, \tag{4.6}$$

and, under strongly non-hydrostatic conditions, by

$$\lim_{\substack{x\to\infty \\ \delta\to 0}} \sigma^2 = \frac{Ri-1}{\delta^2}. \tag{4.7}$$

As for the 'geostrophic' instabilities, the growth rates of symmetric instabilities are decreased by non-hydrostatic effects, but in this case the effect is important when $\delta \sim 1$, not only when $\delta \gg 1$.

For finite x and λ, the growth rates decrease, falling monotonically to zero at

$$x^2 = \frac{1}{1-Ri}. \tag{4.8}$$

The dependence of growth rate on meridional wave-number for the symmetric instabilities is illustrated in figure 2. The curves are plotted for $Ri = \frac{1}{2}$, but the qualitative behaviour would be no different for other values of Ri, so long as $0 < Ri < 1$. The depression of the growth rates under non-hydrostatic conditions is readily apparent from a comparison of the curves for $\delta = 0$, 1, and 2 in figure 2. The total x dependence of the growth rate under strongly non-hydrostatic conditions is given by

$$\lim_{\delta\to\infty} \sigma^2 = \frac{1-x^2(1-Ri)}{\delta^2 x^2}. \tag{4.9}$$

One can easily show that the most rapidly growing symmetric perturbation ($\lambda = \infty$, $k = 0$) always corresponds to a local maximum in $\sigma_i(k, \lambda)$ by using the same method as in §3 of I. In particular, one expands the solution to (2.25) in series of the form,

$$\sigma = \sigma_0 + \frac{\sigma_1(k\lambda^2)}{\lambda^2} + O\left(\frac{1}{\lambda^3}\right), \tag{4.10}$$

and then examines the first-order solution to see how the growth rate changes for the non-symmetric perturbations, $k > 0$. The expansion leads to a first-order equation of exactly the same form as (3.20) in I, except that now the coefficients depend on δ. Since the analysis of (3.20) in I did not depend on the values of the coefficients, the same result applies under non-hydrostatic conditions, namely, $\sigma_i(k, \lambda)$ has a local maximum at $k = 0$, $\lambda = \infty$ when $Ri < 1$.

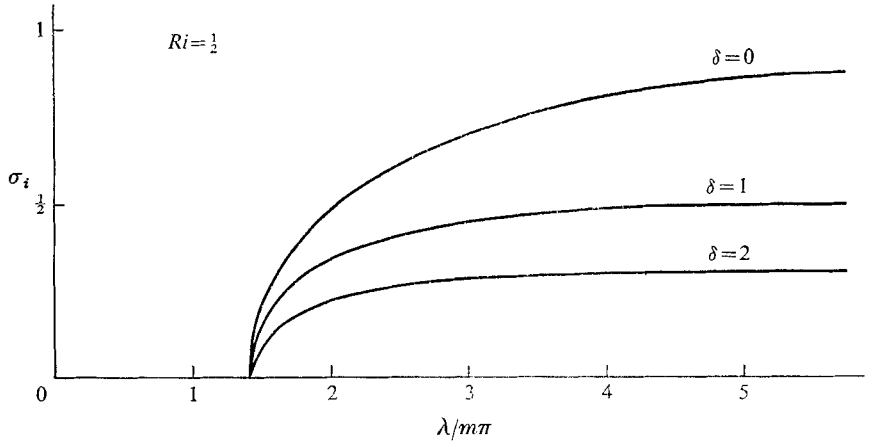

FIGURE 2. Growth rate against meridional wave-number for symmetric instabilities under hydrostatic ($\delta = 0$) and non-hydrostatic ($\delta = 1, 2$) conditions.

Finally, we note that non-hydrostatic conditions do lead to one important change in the eigenfunction for the most rapidly growing symmetric instabilities. From the solution (4.2), we find that the meridional stream function for this mode is given by

$$\phi = \exp\left\{\sigma_i t + i\lambda\left(y - \frac{z}{1+\sigma_i^2}\right)\right\}\sin m\pi z. \tag{4.11}$$

This stream function corresponds to overturning cells with slanting sides of slope

$$dz/dy = 1 + \sigma_i^2. \tag{4.12}$$

Since non-hydrostatic effects decrease the growth rates, the slope of the cells is decreased under non-hydrostatic conditions. The maximum growth rate occurs when $\delta = 0$, $x = \infty$, and corresponds to $1 + \sigma_i^2 = 1/Ri$ (cf. (4.6)). This is just the slope of the isotherms in the basic flow field (cf. (2.17)). Consequently, the slope of the meridional cells is always less than the slope of the isotherms.†

5. Kelvin–Helmholtz instability

According to the results of I, this type of instability is associated with relatively small-scale perturbations ($k \gg 1$) and has relatively large growth rates ($\sigma_i \sim k$). Therefore, we substitute (3.1) and (3.5) into (2.25) and let $k \to \infty$,

† The statement in Stone *et al.* (1969) that the slope of the cells is greater than the slope of the isotherms under non-hydrostatic conditions is in error.

assuming that Ri, ϵ and c are all of order unity, and that $\lambda \lesssim k$. The eigenvalue equation becomes

$$\frac{d^2w}{dz^2} + \left(1 + \frac{\lambda^2}{k^2}\right)\left[\frac{Ri}{(z+c)^2} - \epsilon^2\right] w = 0. \tag{5.1}$$

In this limit of large Rossby number ($k \gg 1$), all rotational effects have completely disappeared from the eigenvalue equation, and it has reduced to the form studied by Eliassen, Hoiland & Riis (1953). (In their model $\lambda = 0$, but their results also apply to (5.1) if we simply redefine Ri and ϵ in an appropriate manner.) Unfortunately, a model of Kelvin–Helmholtz instability like theirs and ours, which has uniform shear in the basic flow (see (2.16)), does not give results typical of the same problem with an arbitrary flow profile. The problem for a shear flow with a general profile has been discussed in some detail by Drazin & Howard (1966, §5). Thus, in order to make a physically meaningful comparison with the results of §§3 and 4, we shall use the results described by Drazin & Howard, rather than those of Eliassen *et al.*

In particular, for realistic shear flows (i.e. those with non-uniform shear and no discontinuities), Kelvin–Helmholtz instability occurs whenever

$$Ri < \tfrac{1}{4}. \tag{5.2}$$

In this criterion, Ri should be interpreted as the local value of the Richardson number, the value obtained by substituting $\partial u/\partial z$ for u_0/H in the definition (2.13). Quantitative values of the unstable wave-numbers and growth rates depend on the actual profile of the shear flow, but the qualitative behaviour is the same in all cases. In order of magnitude, the most unstable perturbations are those with infinite meridional scales and zonal scales comparable to the vertical scale of the shear flow,

$$\lambda = 0, \quad k \sim 1/\delta. \tag{5.3}$$

Their complex phase speeds are comparable to the speed of the basic flow, $|c| \sim 1$. Therefore, the order of magnitude of the growth rate is

$$\sigma_i \sim k|c| \sim 1/\delta, \tag{5.4}$$

so long as Ri is not very close to $\frac{1}{4}$.

Equation (5.3) shows that so long as $\delta \ll 1$ our assumption $k \gg 1$ remains valid. Consequently, the effects of rotation will not modify the Kelvin–Helmholtz instabilities, and they correspond to distinctly different kinds of perturbations from the instabilities discussed in §§3 and 4. Since both the symmetric and 'geostrophic' instabilities have growth rates of order unity when $\delta \ll 1$, the Kelvin–Helmholtz instabilities will have much larger growth rates, unless Ri is very close to $\frac{1}{4}$.

However, when $\delta \gtrsim 1$, (5.3) shows that the assumption of large Rossby number ($k \gg 1$) is no longer valid, and the effects of rotation will modify Kelvin–Helmholtz instabilities. For these values of δ, the magnitudes of σ_i, λ and k associated with Kelvin–Helmholtz instability are just the same as those covered by the analysis in §3. That analysis showed that the instability associated with these perturbations is essentially 'geostrophic' instability when $\delta \gtrsim 1$, and therefore the two types of instability are no longer distinct. In general, there will be a critical value of δ_c, which will mark the upper limit of δ for which there exist two distinct maxima in the growth rates for the different perturbations, $k \gtrsim 1$ and $k \lesssim 1$.

δ_c will be of order unity provided that $Ri < \frac{1}{4}$ and that Ri is not too close to $\frac{1}{4}$. In order to determine the exact value of δ_c for different values of Ri, and how the two types of instability merge when $\delta \sim \delta_c$, one would need to study a particular model with non-uniform shear in the basic flow. As we saw in §4, for small values of Ri and δ, the symmetric and 'geostrophic' instabilities are themselves not distinct, and there is a single maximum in the growth rate corresponding to symmetric instabilities. Therefore, the Kelvin–Helmholtz instabilities may merge directly with the symmetric instabilities if δ_c is not too large.

6. Summary

Figure 3 summarizes the results of §§3–5. It shows the different régimes of instability which can occur for different values of the two basic parameters, Ri and δ. The three solid curves represent the boundaries of the regions where

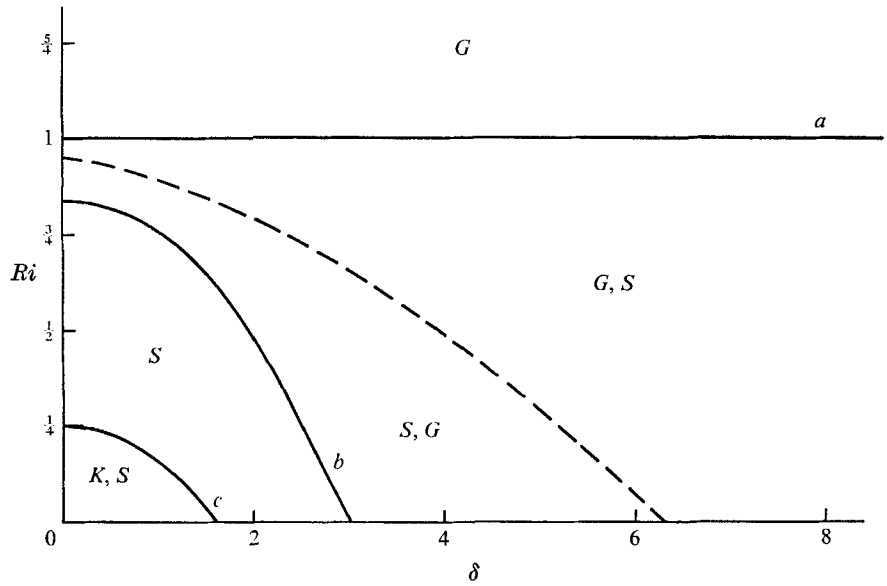

FIGURE 3. Instability régimes in the Ri, δ plane. G stands for 'geostrophic' baroclinic instability, S for symmetric instability, and K for Kelvin–Helmholtz instability. Along the dotted line the maximum growth rates for G and S are equal.

one particular kind of instability can occur, and within each region capital letters designate which kind of instability can occur. G stands for 'geostrophic' instability; S for symmetric instability; and K for Kelvin–Helmholtz instability.

Curve a is the neutral stability criterion for symmetric instability, $Ri = 1$. Symmetric instability can occur anywhere in the diagram below this curve.

Curve b represents the curve along which the growing 'geostrophic' modes cease to have a local growth rate maximum in the (k, λ) plane. This curve is given approximately by (3.24). Actually, in the diagram (3.24) was only used to plot curve b when $\delta \gtrsim 1$. The exact intersection of the curve b with the Ri axis was taken from the results of II, and the curve was interpolated for intermediate

values. 'Geostrophic' instability can occur anywhere in the diagram above curve b.

Curve c represents the curve along which Kelvin–Helmholtz instability ceases to be distinct from the other two kinds of instability. This curve is only indicated schematically, using our conclusion in §5 that it intersects the Ri axis at $Ri = \frac{1}{4}$, and the δ-axis at a value of order unity. To delineate this curve more accurately would require a model with non-uniform shear in the flow. The results of such a model might show that curves b and c actually cross. If so, there would be a régime adjacent to the δ-axis and between these two curves b and c, where all three kinds of instability could occur. Kelvin–Helmholtz instability can occur anywhere in the diagram below curve c.

The dotted line in figure 3 represents the curve along which the largest growth rates for symmetric and 'geostrophic' instability are equal. This curve was computed numerically by equating the two expressions for the maximum growth rate, (3.12) (evaluated for the value of k given by (3.13)) and (4.5). Above the dotted line, 'geostrophic' baroclinic instabilities grow more rapidly, while below it symmetric instabilities grow more rapidly.

Because of all the approximations made in deriving the results displayed in figure 3, its quantitative features should not be taken too seriously. Rather, figure 3 is meant to illustrate schematically what kinds of flow régimes can occur in a baroclinic flow. In general, finite values of δ (which, according to definition (2.14) may be interpreted as either a non-hydrostatic or a rotational effect) tend to suppress symmetric and Kelvin–Helmholtz instability relative to 'geostrophic' baroclinic instability. The deviations also tend to broaden the parameter range in which symmetric and 'geostrophic' baroclinic instability can occur simultaneously.

If one does not neglect dissipative effects, McIntyre (1969) has shown that two further kinds of symmetric baroclinic instability can occur. These 'diffusive' instabilities generally have smaller scales than the kinds of instability we have discussed. Also, they have smaller growth rates, so long as the Prandtl number is not greatly different from unity. However, they can have larger growth rates if the Prandtl number is either extremely small or extremely large.

In realistic geophysical situations, $\delta \ll 1$, so our main motivation has been to determine how laboratory studies of the various kinds of baroclinic instability will be affected by deviations from hydrostatic equilibrium. It is apparent from figure 3 that a laboratory study of symmetric instability should be designed so that $\delta \lesssim 1$, and a laboratory study of Kelvin–Helmholtz instability should be designed so that $\delta \ll 1$. Consequently, it is of interest to estimate the value of δ in the experiments reported by Stone *et al.* (1969),which did contain symmetric instabilities.

The definition of δ, (2.14), can be written in more convenient form if we use the thermal wind relation to write u_0 in terms of the horizontal temperature gradient. It is also convenient to write the horizontal and vertical temperature gradients in terms of the slope of the temperature field,

$$s = (dz/dy)_T, \tag{6.1}$$

and the total temperature contrast Δ across a section of the fluid with horizontal and vertical scales L and H. The resulting expression for δ is

$$\delta = \frac{4\Omega^2(H+sL)}{\alpha g \Delta s}. \tag{6.2}$$

Stone *et al.* (1969) did not report measurements of s, but they did report the slope of the overturning symmetric cells. The results of §4 showed that the slope of the cells is always less than s, and therefore we have a lower bound on s, and this in turn will give an upper bound on δ. Using the figures quoted by Stone *et al.* (1969), for their two pictures illustrating well-developed symmetric overturning, we find

$$\left.\begin{aligned} \delta &\leqslant 0{\cdot}06 \quad \text{(their figure 4)}, \\ \delta &\leqslant 0{\cdot}2 \quad \text{(their figure 5)}. \end{aligned}\right\} \tag{6.3}$$

Consequently, hydrostatic equilibrium should be a good approximation for their experiment. In fact, the different instability régimes they observed agree qualitatively with what one would expect from figure 3 when $\delta \ll 1$.

I am indebted to the Department of Astro-Geophysics at the University of Colorado for their hospitality while a part of this research was carried out. This research was supported in part by the Atmospheric Sciences Section, National Science Foundation, under grant GP–4293 to Harvard University, and in part by a grant from the Alfred P. Sloan Foundation.

REFERENCES

CHARNEY, J. G. 1947 The dynamics of long waves in a baroclinic westerly current. *J. Meteor.* **4**, 135–162.

DRAZIN, P. G. & HOWARD, L. N. 1966 Hydrodynamic stability of parallel flow of inviscid fluid. *Advanc. appl. Mech.* **9**, 1–89.

EADY, E. T. 1949 Long waves and cyclone waves. *Tellus*, **1**, 33–52.

ELIASSEN, A., HOILAND, E. & RIIS, E. 1953 Two-dimensional perturbation of a flow with constant shear of a stratified fluid. *Publications of the Norwegian Academy of Sciences and Letters* (Series W), no. 1, 30 pp.

FOWLIS, W. W. & HIDE, R. 1965 Thermal convection in a rotating annulus. *J. Atmos. Sci.* **22**, 541–558.

FULTZ, D., LONG, R. R., OWENS, G. V., BOHAN, W., KAYLOR, R. & WEIL, J. 1959 Studies of thermal convection in a rotating cylinder. *Meteor. Monogr.* **4**, 1–104.

MCINTYRE, M. E. 1969 Diffusive destabilization of the baroclinic circular vortex. *Geophysical Fluid Dynamics*, **1**, 19–58.

PHILLIPS, N. A. 1963 Geostrophic motion. *Rev. Geophys.* **1**, 123–176.

SOLBERG, H. 1936 Le Mouvement d'Inertie de l'Atmosphère Stable et son Rôle dans la Théorie des Cyclones. *Proc.-verb. Assc. Météor. U.G.G.I.* (Edinburgh), part II (Mém.), pp. 66–82.

STONE, P. H. 1966 On non-geostrophic baroclinic stability. *J. atmos. Sci.* **23**, 390–400.

STONE, P. H. 1970 On non-geostrophic baroclinic stability. Part II. *J. atmos. Sci.* **27**. (To be published.)

STONE, P. H., HESS, S., HADLOCK, R. & RAY, P. 1969 Preliminary results of experiments with symmetric baroclinic instabilities. *J. atmos. Sci.* **26**, 991–996.